

See discussions, stats, and author profiles for this publication at: <https://www.researchgate.net/publication/383718614>

FLEXURAL WAVE PROPAGATION ANALYSIS OF A LOCALLY RESONANT BEAM

Conference Paper · August 2024

DOI: 10.26678/ABCM.CONEM2024.CON24-1502

CITATIONS

0

READS

163

3 authors:



Jenario Souza dos Reis Júnior

Federal University of Piauí

3 PUBLICATIONS 5 CITATIONS

SEE PROFILE



Isadora de Souza

Federal University of Piauí

1 PUBLICATION 0 CITATIONS

SEE PROFILE



Simone dos Santos

Federal University of Piauí

31 PUBLICATIONS 79 CITATIONS

SEE PROFILE

See discussions, stats, and author profiles for this publication at: <https://www.researchgate.net/publication/383718614>

FLEXURAL WAVE PROPAGATION ANALYSIS OF A LOCALLY RESONANT BEAM

Conference Paper · August 2024
 DOI: 10.26678/ABCM.CONEM2024.CON24-1502

CITATIONS
 0

READS
 136

3 authors:



Jenario Souza dos Reis Júnior

Federal University of Piauí

2 PUBLICATIONS 2 CITATIONS

SEE PROFILE




Isadora de Souza

Federal University of Piauí

1 PUBLICATION 0 CITATIONS

SEE PROFILE



Simone dos Santos

Federal University of Piauí

30 PUBLICATIONS 78 CITATIONS

SEE PROFILE

CONEM2024-1502

FLEXURAL WAVE PROPAGATION ANALYSIS OF A LOCALLY RESONANT BEAM

Jenário Souza dos Reis Júnior, jenariojunior4@gmail.com¹
Isadora Rodrigues de Souza, irs08902@gmail.com¹
Simone dos Santos Hoefel, simone.santos@ufpi.edu.br¹

¹Federal University of Piauí, Campus Universitário Ministro Petrônio Portella - Ininga, 64049-550, Teresina PI, Brazil

Abstract: *Metamaterials have become a topic of considerable interest in the scientific and engineering communities in recent decades. Such artificially designed structures offer innovative solutions to complex problems related to wave propagation and vibration control, and have enormous potential for applications in various engineering fields. A topic that has received considerable attention in recent years is the ability to enhance emerging bandgaps due to Bragg scattering and local resonance, and thus improve the wave filtering ability of metamaterials. The present article proposes to analyze a locally resonant Euler-Bernoulli beam that is coupled to a large number of resonators with multiple degrees of freedom that are periodically distributed throughout the structure in order to increase the areas where wave attenuation is observed. Wave and Finite Element Method is applied in order to obtain the dispersion relation for wave propagation for the analysis of wave attenuation mechanisms. The results indicate the pronounced presence of Bragg scattering bandgaps and local resonance bandgaps. The influence of increasing the number of resonators is analyzed, resulting in an increase in the number of bandgaps. Effects of varying the length of the periodic unit on the attenuation property are also investigated. An increase of this parameter leads to an increment of the maximum attenuation coefficient and a new bandgap of the Bragg scattering is observed. In addition, the bandgap behavior is examined when the periodicity due to the presence of resonators is harmonized with the material periodicity, resulting from the use of two materials per unit cell. Finally, the vibration transmittance is determined by means of the classical Finite Element Method. The results of the vibration transmission show that the wave attenuation appears in the same frequency bands as those obtained by the Wave and Finite Element Method, which corroborates the efficient wave filtering performance of the locally resonant metamaterial beam.*

Keywords: *Locally resonant metamaterial, Flexural wave attenuation, Complex band structure, Wave and Finite Element Method, Bandgaps.*

1. INTRODUCTION

Structural vibrations affect the maintenance and safety of buildings and facilities, requiring the implementation of vibration isolation and suppression measures. Using metamaterials, macroscopic composites of periodic or non-periodic structures that perform specific functions based on their cellular architecture and chemical composition (Smith *et al.*, 2010), is a possible measure. According to Sun *et al.* (2010), this new class of composites proposed by the Defense Advanced Research Projects Agency (DARPA) in 2001 aims to showcase exceptional material properties not found in nature or its constituents. Xiao *et al.* (2012) explain that metamaterials can filter waves due to the presence of frequency bands or energy bands where waves cannot propagate. Such regions, known as bandgaps, have a significant impact on the mechanical, thermal and acoustic properties of the material.

Bandgaps are generated by two types of mechanisms: Bragg scattering or local resonance. Bragg scattering bandgap (BSBG) emerges due to destructive interference between incident and reflected waves that occur when the wavelengths are of the same order as the dimension of the periodic units (Silva *et al.*, 2016). Local resonance bandgap (LRBG) can be generated at wavelengths that are much larger than the size of the grating, thus allowing for the attenuation of low frequency vibrations (El-Borgi *et al.*, 2020). Metamaterials have numerous engineering applications due to their unique ability to reduce wave propagation, exemplified by their utilization as a waveguide, a fact which is highlighted by Broadman *et al.* (2021). In addition, it is effective in the development of metabarriers, evidenced by Lim *et al.* (2021), and in the development of metasurfaces, as shown by Carneiro *et al.* (2023), for the reduction of vibrations transmitted

through the ground, such as seismic waves. It also has the potential to reduce aircraft noise (Moruzzi *et al.*, 2021) and to reduce underwater noise caused by the installation of offshore monopiles (Vasconcelos *et al.*, 2024).

The concept of metamaterials extends to periodic structures coupled with locally resonant devices that act as absorbers for mechanical vibrations (Huang and Sun, 2010). An example is the research of Wang *et al.* (2005), who analyzed the propagation of longitudinal waves in a rod coupled to resonators. Another relevant work is that of Xiao *et al.* (2012), investigated a metamaterial rod with multiple degrees of freedom (MDOF) resonators, which resulted in the introduction of multiple local resonance bandgaps. Zhu *et al.* (2014) demonstrated that multiple resonators with different natural frequencies can also achieve this effect. To improve certain characteristics of bandgaps, Fang *et al.* (2017) proposed the incorporation of nonlinearity, which led to the observation of new bandgaps based on the chaos mechanism. Khajehtou-rian and Hussein (2014) presented a study on a nonlinear metamaterial rod with periodically coupled local resonators, and demonstrated that a large deformation can induce a pair of Bragg bandgaps and merge resonances, forming a wide combined bandgap.

Several numerical methods have been developed to analyze metamaterial properties. More recently, Wang *et al.* (2023) performed a Spectral Element Method work on prestressed metamaterial beams coupled to local resonators connected by piezoelectric springs, and found that as the number of resonators increases, the amount of local resonance bandgaps also increases. Miranda Jr *et al.* (2019) utilized the Plane Wave Expansion Method to study the effects of local resonators with MDOF on elastic metamaterial plates, considering the Kirchhoff-Love thin plate theory. An alternative employed approach is the Wave and Finite Element Method (WFEM), utilized for solving complex wave propagation problems. This method significantly reduces the model size compared to a complete finite element model. In this paper, the analysis focuses on a locally resonant (LR) beam coupled with various periodically distributed resonators. The beam element is formulated based on the Euler-Bernoulli theory and discretized using the Finite Element Method (FEM). Three numerical examples are presented in order to analyze the frequency ranges in which the waves are attenuated. The investigation of bandgaps behavior considering variations in geometric and material parameters is performed by analyzing the dispersion curves and the vibration transmittance obtained by WFEM and conventional FEM, respectively.

2. DESCRIPTIONS OF MODEL

The Euler-Bernoulli beam periodically fixed by resonators, as shown in Fig. 1a, is considered in this study. Each resonator consists of a mass connected to the beam by a spring. The dimensions of the beam are given by the width b and thickness h . The model of the beam can be represented by an infinite set of unit cells. Figure 1b presents a unit cell of the structure with n resonators and n springs without mass attached to the beam, where the length of the unit cell, also referred to as the lattice constant, is represented by a and the mass of resonators and springs stiffness constant of the structure are denoted by m_i and k_i , respectively, where $i = 1, 2, 3, \dots, n$.

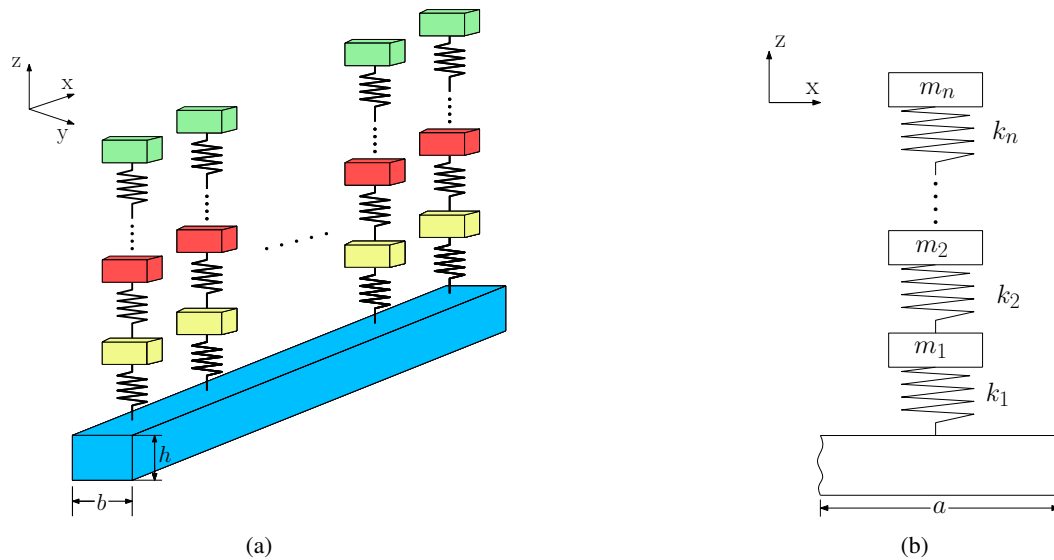


Figure 1: Illustrative diagram of the LR beam and the unit cell of the structure.

3. DISPERSION CURVES CALCULATION

Dispersion curves or dispersion relations demonstrate the correlation between angular frequency and propagation constants and elucidate the wave propagation in the corresponding infinite periodic structure. Numerical approaches, such as the WFEM, have been extensively used to compute the dispersion relations for complex periodic structures. This method was formulated to evaluate the dynamic responses of periodic structures and waveguides (Mace *et al.*, 2005) and can be utilized as a condensed representation for complex structures. WFEM is also a computational technique that merges the adaptability of the FEM with Floquet-Bloch theory to determine the dispersion characteristics of a periodic

medium by analyzing stiffness and mass matrices, determined using standard FEM for a unit cell of the structure, and processing these matrices with enforced periodicity conditions to model the wave propagation across the structure. For each unit cell, Fig. 2 shows the partitioning of degrees of freedom and force equilibrium:

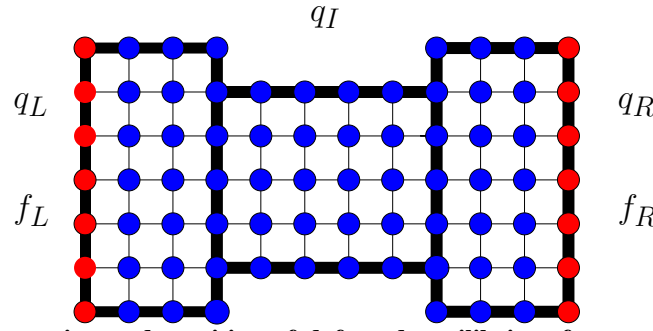


Figure 2: **Schematic representation and partition of dofs and equilibrium forces of a unit cell of a infinite 1D periodic structure.**

where \mathbf{q}_L , \mathbf{q}_I and \mathbf{q}_R correspond to left boundary, internal and right boundary degrees of freedom, respectively, and \mathbf{f}_L and \mathbf{f}_R correspond to left boundary and right boundary equilibrium forces, respectively.

Applying the finite element technique, the substructure's equation of motion, assuming harmonic time behavior and neglecting damping, can be expressed in matrix notation as:

$$[\mathbf{K} - \omega^2 \mathbf{M}] \mathbf{q} = \mathbf{f}, \quad (1)$$

where \mathbf{K} corresponds to the stiffness matrix, ω to the angular frequency, \mathbf{M} to the mass matrix, \mathbf{q} is the vector of degrees of freedom of the considered structure and \mathbf{f} is the vector of nodal loads.

The Bloch-Floquet theorem can be applied due to the periodicity of the structure, enabling the expression of physical parameters at the boundaries of each unit cell as follows:

$$\mathbf{q}_R = \mathbf{q}_L \lambda, \quad (2)$$

$$\mathbf{f}_R = -\mathbf{f}_L \lambda, \quad (3)$$

where λ is the Bloch (Floquet)-propagator, which is related to the propagation constant μ by:

$$\lambda = e^{i\mu} \quad \text{and} \quad \mu = ka, \quad (4)$$

in which $i = \sqrt{-1}$ and k is the wavenumber.

Determining the band structure typically requires solving an eigenvalue problem. Based on the formulation of eigenvalue problems, these can be grouped into direct and inverse approaches.

3.1 The Inverse Approach $\omega(\mu)$

Real wave propagation constants μ are imposed in the inverse method to obtain angular frequencies (Cool *et al.*, 2022). By applying Bloch's theorem, given by Eqs. (2) and (3), to the unit cell boundaries and accounting for the propagation of plane waves in the structure, periodic boundary conditions are implemented, resulting in:

$$\mathbf{q} = \Lambda \tilde{\mathbf{q}}, \quad (5)$$

which $\tilde{\mathbf{q}}$ is the periodic degree of freedom vector, and Λ is the periodicity matrix of the following form by (Beli *et al.*, 2018):

$$\mathbf{q} = [\mathbf{q}_L \quad \mathbf{q}_I \quad \mathbf{q}_R]^T, \quad \tilde{\mathbf{q}} = [\mathbf{q}_L \quad \mathbf{q}_I]^T, \quad \Lambda = \begin{bmatrix} \mathbf{I} & \mathbf{0} & \lambda \mathbf{I} \\ \mathbf{0} & \mathbf{I} & \mathbf{0} \end{bmatrix}^T, \quad (6)$$

where \mathbf{T} indicates the transpose of the matrix. In the absence of external forces, the force equilibrium is expressed in matrix form as:

$$\Lambda^H \mathbf{f} = \mathbf{0}, \quad (7)$$

where \mathbf{f} represents the vector of generalized boundary forces and \mathbf{H} denotes the Hermitian transpose:

$$\Lambda^H = \begin{bmatrix} \mathbf{I} & \mathbf{0} & \lambda^{-1}\mathbf{I} \\ \mathbf{0} & \mathbf{I} & \mathbf{0} \end{bmatrix}. \quad (8)$$

Multiplying the governing harmonic equation of the unit cell, presented from Eq. (1), by Λ^H on the left-hand side and substituting Eq. (5) in Eq. (1), the stiffness and mass matrices are presented in a simplified basis, and an eigenvalue problem $\omega(\mu)$ is formulated for a defined reciprocal lattice direction, as follows:

$$[\tilde{\mathbf{K}} - \omega\tilde{\mathbf{M}}]\tilde{\mathbf{q}} = \mathbf{0}, \quad (9)$$

which $\tilde{\mathbf{K}}$, $\tilde{\mathbf{M}}$ are a function of μ and given by:

$$\tilde{\mathbf{K}} = \Lambda^H \mathbf{K} \Lambda \quad \text{and} \quad \tilde{\mathbf{M}} = \Lambda^H \mathbf{M} \Lambda. \quad (10)$$

Due to periodicity, the irreducible Brillouin zone (IBZ) contains all pertinent propagation constant details for the infinite periodic structure. Note that the Eq. (9) represents an eigenvalue problem that can be solved for the real propagation constants varying within this domain, that is $\mu \in [0; \pi]$, for the one-dimensional case. However, this procedure fails to yield dispersion curves for the evanescent modes in periodic structures, presenting a significant limitation of the $\omega(\mu)$ approach.

3.2 The Direct Approach $\mu(\omega)$

The angular frequencies are given to determine the wave propagation constants. The direct approach has become significant as it enables the determination of complex band structure for periodic structures and further elucidates the imaginary dispersion structures. This strategy provides the real and imaginary components of propagation constants, which can be utilized to predict, respectively, the propagation and attenuation of flexural waves (Boukadia *et al.*, 2018).

The equation of motion of the unit cell for time harmonic motion at angular frequency ω can be written as:

$$\mathbf{D}(\omega)\mathbf{q} = \mathbf{f}, \quad \mathbf{D}(\omega) = \mathbf{K} - \omega^2\mathbf{M}, \quad (11)$$

where $\mathbf{D}(\omega)$ is the dynamic stiffness matrix, that can be partitioned as:

$$\mathbf{D}(\omega) = \begin{bmatrix} \mathbf{D}_{LL} & \mathbf{D}_{LI} & \mathbf{D}_{LR} \\ \mathbf{D}_{IL} & \mathbf{D}_{II} & \mathbf{D}_{IR} \\ \mathbf{D}_{RL} & \mathbf{D}_{RI} & \mathbf{D}_{RR} \end{bmatrix}. \quad (12)$$

Applying the Bloch boundary conditions, similarly with the inverse method, the Eq. (11) yields:

$$\Lambda^H \mathbf{D}(\omega) \Lambda \tilde{\mathbf{q}} = \mathbf{0}. \quad (13)$$

After some mathematical manipulations, this expression results in a quadratic eigenvalue problem of the following form:

$$[\mathbf{D}_0(\omega) + \lambda\mathbf{D}_1(\omega) + \lambda^2\mathbf{D}_2(\omega)]\tilde{\mathbf{q}} = \mathbf{0}, \quad (14)$$

where:

$$\mathbf{D}_0(\omega) = \begin{bmatrix} \mathbf{D}_{RL} & \mathbf{D}_{RI} \\ \mathbf{0} & \mathbf{0} \end{bmatrix}, \quad \mathbf{D}_1(\omega) = \begin{bmatrix} \mathbf{D}_{LL} + \mathbf{D}_{RR} & \mathbf{D}_{LI} \\ \mathbf{D}_{IL} & \mathbf{D}_{II} \end{bmatrix}, \quad \mathbf{D}_2(\omega) = \begin{bmatrix} \mathbf{D}_{LR} & \mathbf{0} \\ \mathbf{D}_{RI} & \mathbf{0} \end{bmatrix}. \quad (15)$$

The eigenvalues λ for each given ω can be obtained by solving the dispersion eigenvalue problem of the Eq. (14), varying the frequency in the range of interest $\omega \in [0; \omega_{max}]$.

4. VIBRATION TRANSMITTANCE OF FINITE STRUCTURES

Vibration transmittance is extensively investigated to analyze the effectiveness of finite structures in filtering and attenuating vibrations. Considering a metamaterial beam system composed of n unit cells shown in Fig. 3, an external excitation load is applied at the right end of the beam and the displacement vibration response is measured at both ends, where the notations of “Point A” and “Point B” indicate the locations of interest for the transverse vibration responses. Conventional finite element method can be employed to obtain transverse vibration transmittance of such a finite structure. Transmittance T is expressed as follows (Guo *et al.*, 2023):

$$T = 20 \log_{10} \left(\frac{|w_A|}{|w_B|} \right), \quad (16)$$

where w_B and w_A correspond to the transversal displacement of the exciting point and the transversal displacement of the pick-up point in the beam, respectively.

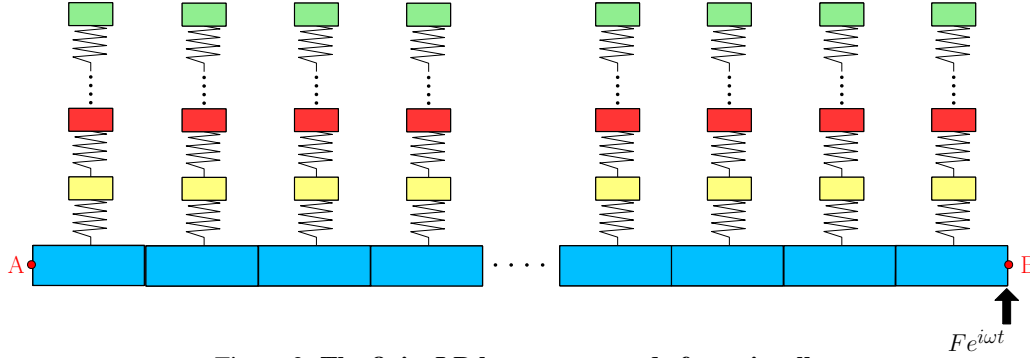


Figure 3: The finite LR beam composed of n unit cells.

5. NUMERICAL RESULTS

In this section, the numerical investigation of the propagation characteristics of flexural waves in an infinite LR beam connected with MDOF resonators will be conducted. The effects of number of resonators per unit cell, based on literature example (Wang *et al.*, 2023 and Zhou *et al.*, 2019), is presented and the impact of unit cell length and combination of materials in unit cell on the bandgaps characteristics are examined. The material parameters of the LR beam and the resonators are defined as follows: $E = 76.92$ GPa, $\rho = 2700$ kg/m³, $k_i = 9.593 \times 10^4$ N/m and the sum of all the masses of the resonators connected to the beam in the unit cell is given by $m = \gamma \rho A a$, where $\gamma = 0.5$ denotes the mass ratio, which represents the ratio of resonator mass to the beam unit cell mass, and A is the sectional area of the beam. Table 1 lists the geometric parameters of the LR beam. The parameters h , b and γ are considered constants for all analyses performed in this study.

Table 1: Geometric parameters of a LR beam.

h (m)	b (m)	a (m)
0.002 m	0.1	0.1

5.1 Effects of the Number of Resonators

In order to investigate the influence of the number of resonators on the bandgaps behavior, the dispersion curves of the LR beam considering 1, 2 and 3 resonators per unit cell is showed in Figs. 4-6, respectively. The distribution of resonator masses is presented in Tab. 2. These complex band structures represent the relationship between frequency and constant propagation along the unit cell of structure. The real part of the wave propagation constant μ means freely propagating waves and determined via the $\omega(\mu)$ approach. The imaginary part of μ , known as the attenuation coefficient and evaluated by the $\mu(\omega)$ approach, characterizes the spatial attenuation of amplitude as the wave traverses the lattice.

Table 2: Details of resonator mass.

Number of resonators	Resonator mass (kg)		
	m_1	m_2	m_3
1	0.027	0	0
2	0.01305	0.01305	0
3	0.009	0.009	0.009

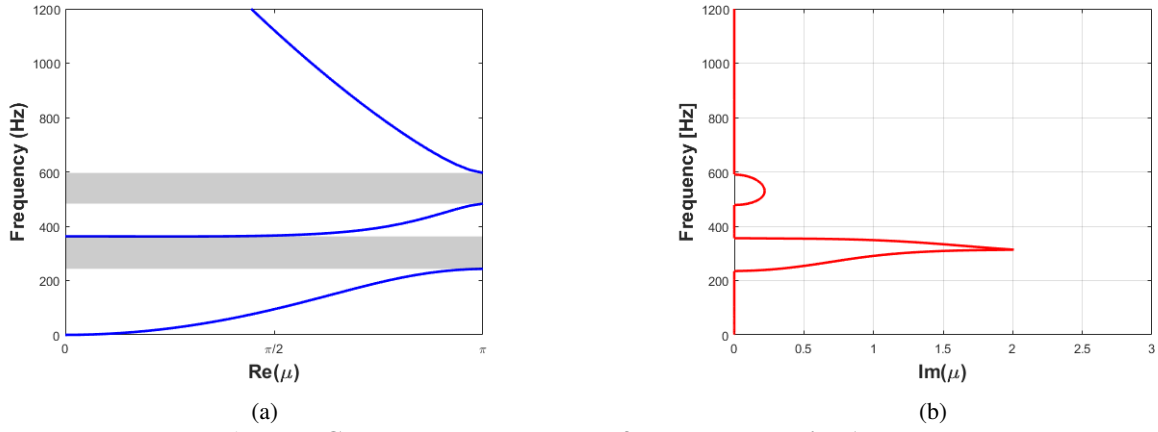


Figure 4: Complex band structure of the LR beam with 1 resonator.

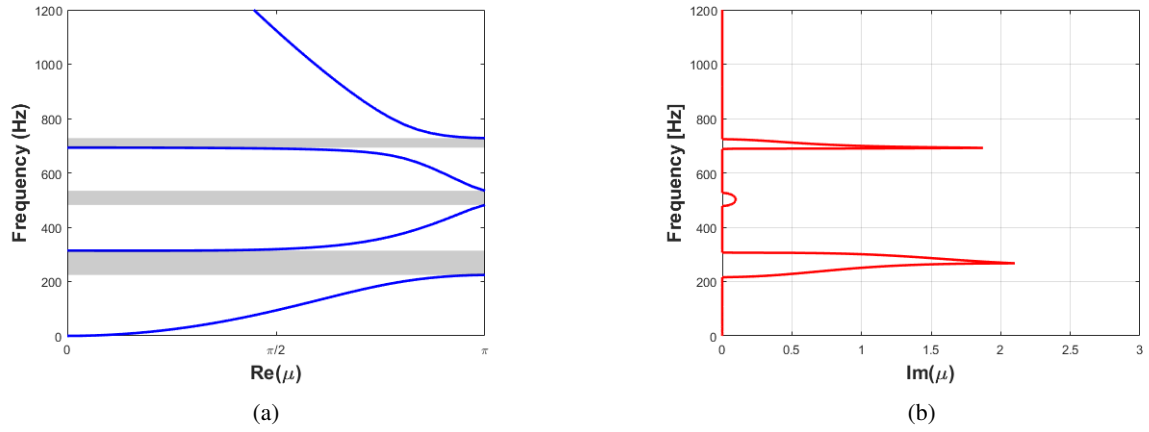


Figure 5: Complex band structure of the LR beam with 2 resonators.

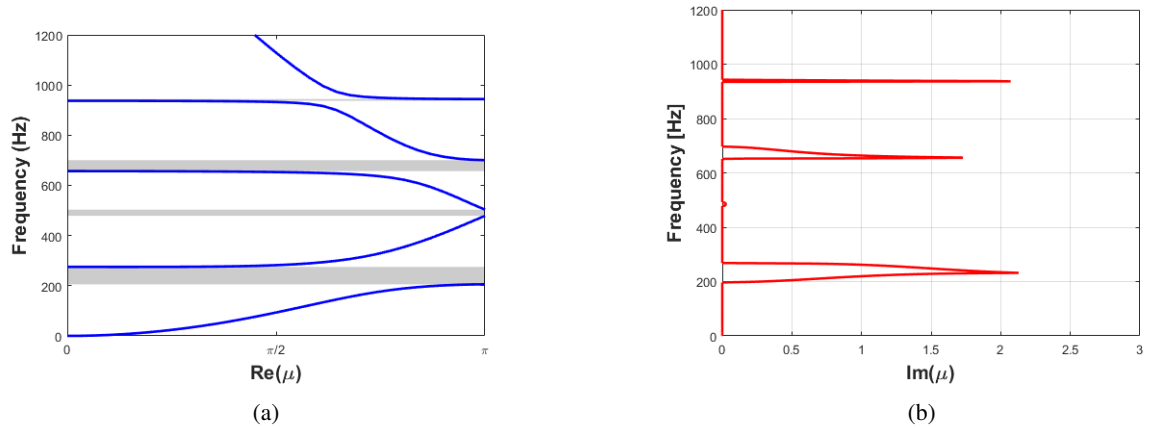


Figure 6: Complex band structure of the LR beam with 3 resonators.

Dispersion curves presented in the Figs. 4-6a evidenced several bandgaps, the gray shaded regions, characterized by frequency ranges where flexural wave propagation is prohibited or significantly attenuated. Figures 4-6b show the attenuation characteristics of flexural waves in the LR beam. The alignment observed between the bandgap intervals and the nonzero values of the attenuation coefficient validates the effective inhibition of flexural wave propagation within the bandgap range. Note that Figs. 4-6b show the presence of two types of bandgaps: LRBG and BSBG. The first is characterized by a sharp peak in attenuation around the natural frequency of the resonators, while the second exhibits a notably smooth attenuation profile across the gap range. Furthermore, it is evident that the addition of a resonator results in the emergence of a new bandgap, with the number of resonators consistently matching with the number of LRBG. A single BSBG persists regardless of the number of attached resonators. These results are in good agreement with literature.

5.2 Effects of the Unit Cell Length and the Material Combinations

Now, the impact of the unit cell length in the characteristics of bandgaps is analysed. Complex band structures were obtained for LR beams, attached with two resonators of equal mass in each unit cell, with $a = 0.075$ m and $a = 0.135$ m, and compared with the case of $a = 0.1$ m (Fig. 5).

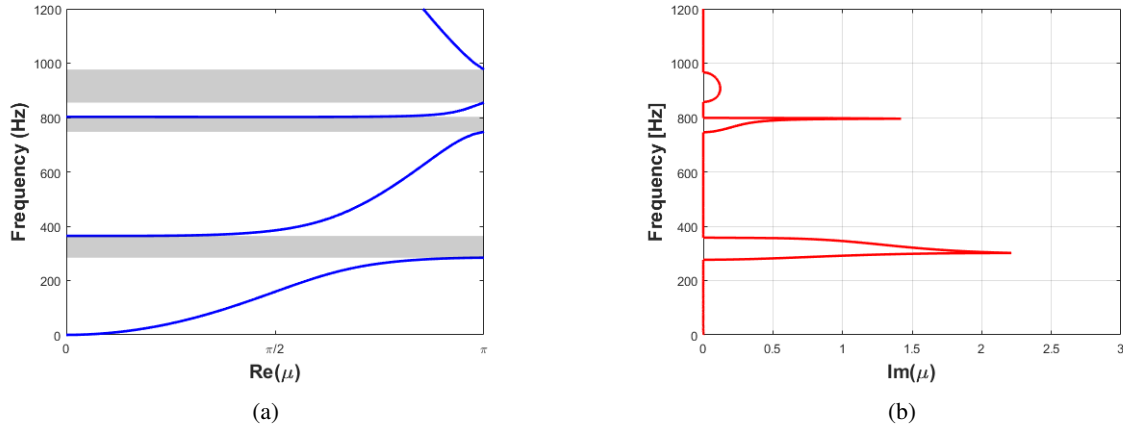


Figure 7: **Complex band structure of the LR beam with different unit cell length: 0.075 m.**

According to dispersion curves showed in Fig. 5, notice that there are two LRBG (215.8-309.6 Hz and 687.6-727 Hz) and one BSBG (478-529.4 Hz) in the frequency range considered. The reduction in the unit cell length from 0.1 m to 0.075 m results in a shift of the BSBG towards a higher frequency range (857-968 Hz) and the width of this bandgap increases considerably. Additionally, the total LRBG (276.3-361 Hz and 745-800.7 Hz) width is increased from 133.2 Hz to 140.4 Hz, as showed in Fig. 7.

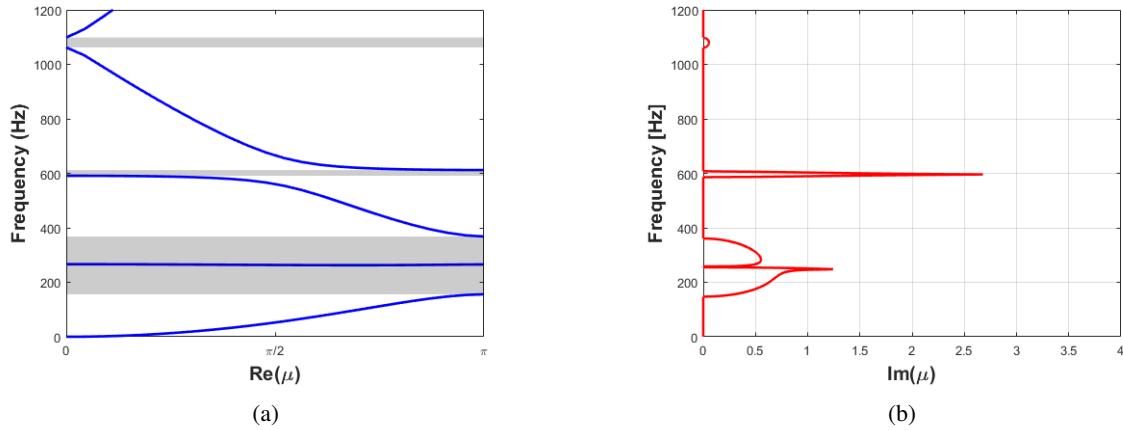


Figure 8: **Complex band structure of the LR beam with different unit cell length: 0.135 m.**

In agreement with the complex band structure presented in the Fig. 8, when the lattice constant is increased to 0.135 m, observe that the emergence of a new BSBG (1061-1099 Hz). Notice that the lower BSBG (258-363 Hz) seems to integrate with the first LRBG. This occurrence of nearly coupled resonance-Bragg gap arises in such a unique circumstance resembling a pseudo-wide gap, given the presence of only an extremely narrow pass band within the gap (Xiao *et al.*, 2013). Note that, as the unit cell length decreases or increases, the BSBG of the band structure shifts to higher or lower frequencies, respectively. The total LRBG (147-256 Hz and 586-612 Hz) width shows a slight increase from 133.2 Hz to 135 Hz, and the maximum attenuation coefficient observed is increased from 2.101 to 2.677. This indicates that as the unit cell length increases, the attenuation of narrower LRBG bands becomes more effective.

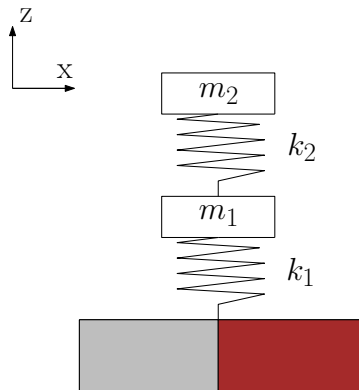


Figure 9: **The unit cell of LR beam with two materials.**

The performance of bandgap behavior is examined, considering now the material combinations in the unit cell of the LR beam. A unit cell where the beam is composed of two different materials and attached with 2 resonators is presented in the Fig. 9. The material parameters considered are listed in Tab. 3 and the geometric parameters correspond to those showed in Tab. 1. Three configurations of materials are investigated: brass-brass, brass-nylon and brass-copper. Figures 10-12 present the dispersion curves for these three cases studied, respectively.

Table 3: **Material parameters.**

Material	Young's modulus (Pa)	Density (kg/m ³)
Brass (Hu <i>et al.</i> , 2023)	100×10^9	7165
Nylon (Gao <i>et al.</i> , 2019)	2×10^9	1150
Copper (Xiao <i>et al.</i> , 2013)	1.65×10^{11}	8700

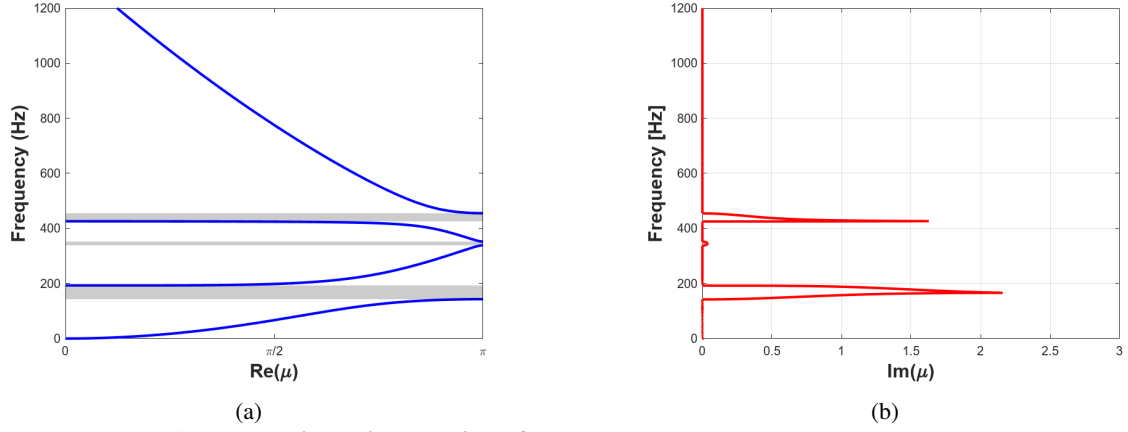


Figure 10: **Dispersion relation of the LR beam composed to brass-brass.**

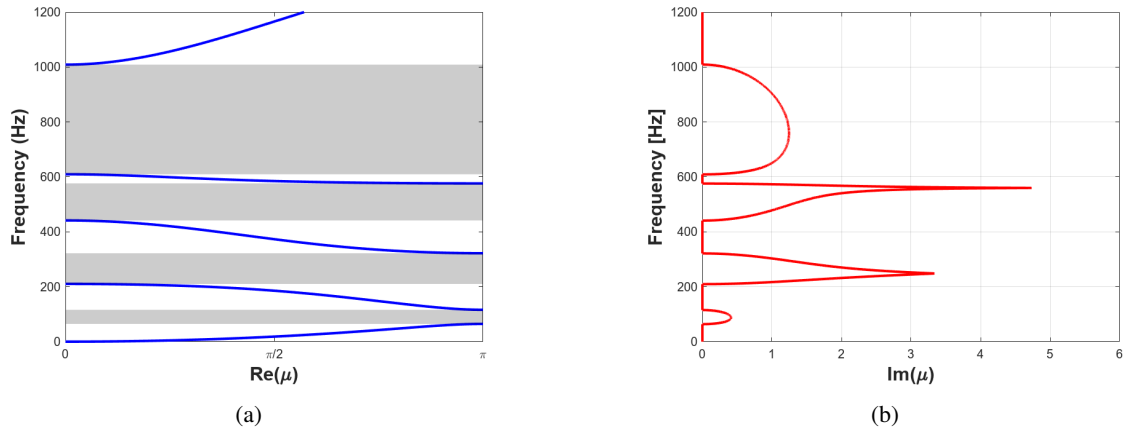


Figure 11: **Dispersion relation of the LR beam with a different material combination (brass-nylon).**

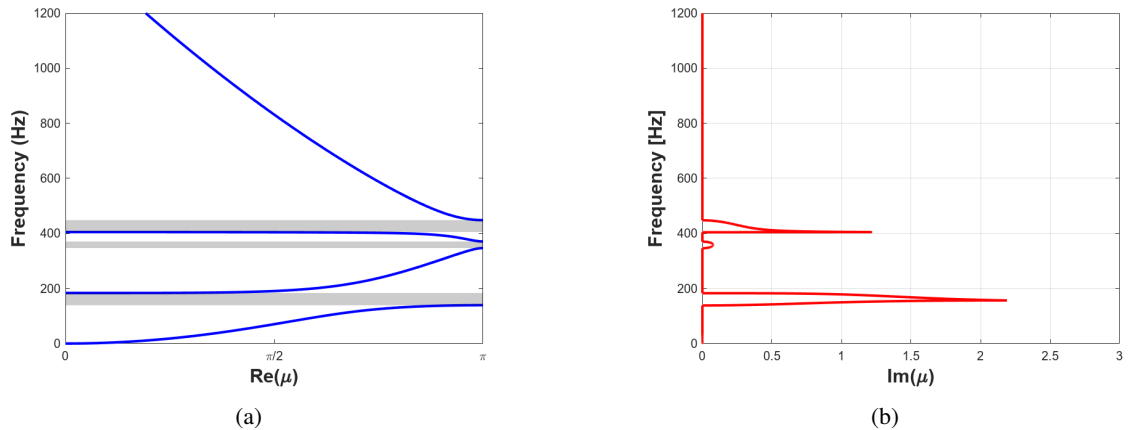


Figure 12: **Dispersion relation of the LR beam with a different material combination (brass-copper).**

Comparing the dispersion relations presented in Figs. 10 and 11, observe that the contrast between these two materials (brass and nylon) results in broader BSBG (609.5-1009 Hz) and enhances the attenuation capability simultaneously. Note that the total bandgap width is increased from 93 Hz to 698 Hz in the analysed frequency range (0-1200 Hz). The use of brass along with heavier materials such as copper, resulted in a small increase in the overall bandgap width, as shown in Fig. 12. The combination of brass with softer materials provides greater attenuation than with harder materials.

5.3 Vibration Transmittance

The previous discussions show that both the length and the materials that compose of the unit cell have a significant effect on the band structure. Figures 13a-b show the vibration transmittance of the LR beam composed of 15, 20 and 30 unit cells. For comparison and generalizability, the unit cells considered in Fig. 13a correspond to the case showed in Fig. 7 and those in Fig. 13b correspond to the case presented in Fig. 11. Based on the smoothly varying attenuation property of the BSBG and the sharply changing attenuation behavior of the LRBG, this approach, employing FEM, can be used as an effective method to identify bandgaps, the gray shaded regions. Notice that the bandgaps become more significant with an increase in the unit cell quantity. These results demonstrate concordance with the range and widths of bandgap obtained from the dispersion curves discussed previously.

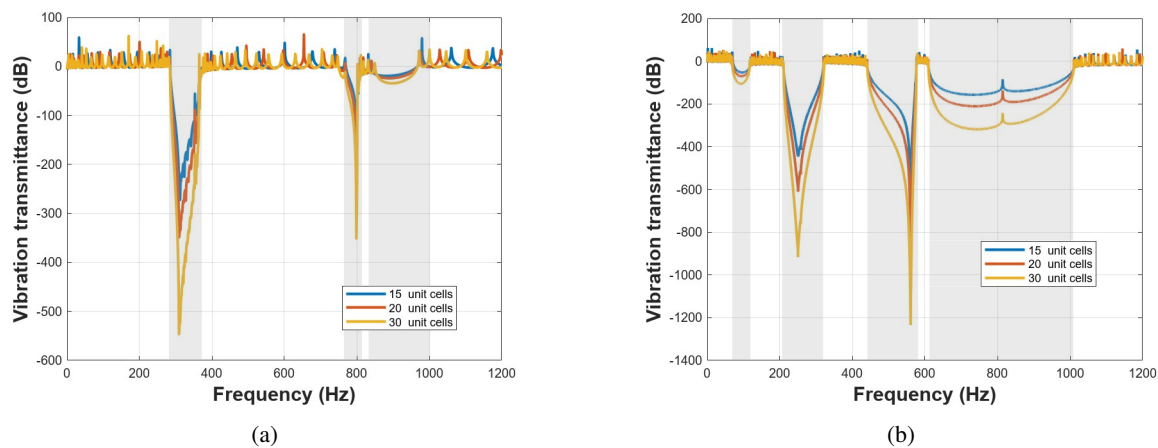


Figure 13: Comparison of vibration transmittance in LR beam with 15, 20 and 30 unit cells considering (a) the unit cell length of 0.075 m and (b) the LR beam composed of brass and nylon.

6. CONCLUSION

Flexural waves propagation in a LR beam consisting of a periodic array of resonators was investigated in this work. WFEM was used to predict the propagation constants and complex band structure of the system. The conventional FEM was employed to determine vibration transmittance. The results highlight the pronounced presence of bandgaps due to Bragg scattering and local resonance. Additionally, it was observed that the number of LRBG can be increased by adding a resonator. Effects of variation of geometric and material parameters were analyzed. Varying the unit cell length, the lower BSBG can be moved to high or low frequency ranges, the quantity of BSBG can be increased and the total LRBG width was modified. Finally, by combining brass with a lighter material in the same unit cell, both the number and width of BSBG are increased, enhancing the attenuation capability. The transmittance vibration analysis, using FEM, is an efficient technique for analyzing the bandgaps of locally resonant beams.

7. REFERENCES

- Beli, D., Arruda, J. and Ruzzene, M., 2018. "Wave propagation in elastic metamaterial beams and plates with interconnected resonators". *International Journal of Solids and Structures*, Vol. 139, pp. 105–120.
- Boukadia, R.F., Droz, C., Ichchou, M.N. and Desmet, W., 2018. "A Bloch wave reduction scheme for ultrafast band diagram and dynamic response computation in periodic structures". *Finite Elements in Analysis and Design*, Vol. 148, pp. 1–12. ISSN 0168-874X.
- Broadman, C.W., Naify, C.J., Lee, M.J. and Haberman, M.R., 2021. "Design of a one-dimensional underwater acoustic leaky wave antenna using an elastic metamaterial waveguide". *Journal of Applied Physics*, Vol. 129, No. 19.
- Carneiro, D., Kabirian Varnosfaderani, Z., Reumers, P., Lombaert, g. and Degrande, G., 2023. "Vibration mitigation using seismic metamaterials on layered soil". *Proceedings of the 12th International Conference on Structural Dynamics, Eurodyn 2023*.
- Cool, V., Naets, F., Van Belle, L., Desmet, W. and Deckers, E., 2022. "Accelerated dispersion curve calculations for periodic vibro-acoustic structures". *Frontiers in Mechanical Engineering*, Vol. 8, p. 995322.
- El-Borgi, S., Fernandes, R., Rajendran, P., Yazbeck, R., Boyd, J. and Lagoudas, D., 2020. "Multiple bandgap formation

- in a locally resonant linear metamaterial beam: Theory and experiments”. *Journal of Sound and Vibration*, Vol. 488, p. 115647.
- Fang, X., Wen, J., Bonello, B., Yin, J. and Yu, D., 2017. “Ultra-low and ultra-broad-band nonlinear acoustic metamaterials”. *Nature communications*, Vol. 8, No. 1, p. 1288.
- Gao, N.S., Guo, X.Y., Cheng, B.Z., Zhang, Y.N., Wei, Z.Y. and Hou, H., 2019. “Elastic wave modulation in hollow metamaterial beam with acoustic black hole”. *Ieee Access*, Vol. 7, pp. 124141–124146.
- Guo, Z., Wen, J., Yu, D., Hu, G. and Yang, Y., 2023. “Widening the Band Gaps of Hourglass Lattice Truss Core Sandwich Structures for Broadband Vibration Suppression”. *Journal of Vibration and Acoustics*, Vol. 145, No. 6, p. 061002. ISSN 1048-9002.
- Hu, G., Tang, L., Yang, Y., Yu, D. and Zi, Y., 2023. “High-fidelity dynamics of piezoelectric covered metamaterial timoshenko beams using the spectral element method”. *Smart Materials and Structures*, Vol. 32, No. 9, p. 095023.
- Huang, H. and Sun, C., 2010. “A study of band-gap phenomena of two locally resonant acoustic metamaterials”. *Proceedings of the Institution of Mechanical Engineers, Part N: Journal of Nanoengineering and Nanosystems*, Vol. 224, No. 3, pp. 83–92.
- Khajehtourian, R. and Hussein, M.I., 2014. “Dispersion characteristics of a nonlinear elastic metamaterial”. *Aip Advances*, Vol. 4, No. 12.
- Lim, C., Žur, K.K. *et al.*, 2021. “Wide Rayleigh waves bandgap engineered metabarriers for ground born vibration attenuation”. *Engineering Structures*, Vol. 246, p. 113019.
- Mace, B.R., Duhamel, D., Brennan, M.J. and Hinke, L., 2005. “Finite element prediction of wave motion in structural waveguides”. *The Journal of the Acoustical Society of America*, Vol. 117, No. 5, pp. 2835–2843.
- Miranda Jr, E., Nobrega, E., Ferreira, A. and Dos Santos, J., 2019. “Flexural wave band gaps in a multi-resonator elastic metamaterial plate using Kirchhoff-Love theory”. *Mechanical Systems and Signal Processing*, Vol. 116, pp. 480–504.
- Moruzzi, M., Cinefra, M. and Bagassi, S., 2021. “Vibroacoustic analysis of an innovative windowless cabin with metamaterial trim panels in regional turboprops”. *Mechanics of Advanced Materials and Structures*, Vol. 28, No. 14, pp. 1509–1521.
- Silva, P., Mencik, J.M. and Arruda, J., 2016. “On the use of the wave finite element method for passive vibration control of periodic structures”. *Advances in Aircraft and Spacecraft Science*, Vol. 3, p. 299–315.
- Smith, D.R., Liu, R. and Cui, T.J., 2010. *Metamaterials: theory, design, and applications*. Springer US.
- Sun, H., Du, X. and Pai, P.F., 2010. “Theory of metamaterial beams for broadband vibration absorption”. *Journal of intelligent material systems and structures*, Vol. 21, No. 11, pp. 1085–1101.
- Vasconcelos, A.C.A., Valappil, S.V., Schott, D., Jovanova, J. and Aragón, A.M., 2024. “A metamaterial-based interface for the structural resonance shielding of impact-driven offshore monopiles”. *Engineering Structures*, Vol. 300, p. 117261.
- Wang, G., Wen, X., Wen, J. and Liu, Y., 2005. “Quasi-One-Dimensional Periodic Structure with Locally Resonant Band Gap”. *Journal of Applied Mechanics*, Vol. 73, No. 1, pp. 167–170.
- Wang, G., Shi, F., Chen, Z., Yu, Y. and Lim, C., 2023. “Controllable flexural wave bandgap in extensible metamaterial beams with embedded multiple resonators”. *Continuum Mechanics and Thermodynamics*, pp. 1–19.
- Xiao, Y., Wen, J. and Wen, X., 2012. “Longitudinal wave band gaps in metamaterial-based elastic rods containing multi-degree-of-freedom resonators”. *New Journal of Physics*, Vol. 14, No. 3, p. 033042.
- Xiao, Y., Wen, J., Yu, D. and Wen, X., 2013. “Flexural wave propagation in beams with periodically attached vibration absorbers: Band-gap behavior and band formation mechanisms”. *Journal of Sound and Vibration*, Vol. 332, No. 4, pp. 867–893.
- Zhou, W., Wu, B., Su, Y., Liu, D., Chen, W. and Bao, R., 2019. “Tunable flexural wave band gaps in a prestressed elastic beam with periodic smart resonators”. *Mechanics of Advanced Materials and Structures*, Vol. 28, pp. 1–8. doi:10.1080/15376494.2018.1553261.
- Zhu, R., Liu, X., Hu, G., Sun, C. and Huang, G., 2014. “A chiral elastic metamaterial beam for broadband vibration suppression”. *Journal of Sound and Vibration*, Vol. 333, No. 10, pp. 2759–2773.

8. RESPONSIBILITY NOTICE

The authors are the only responsible for the printed material included in this paper.